

## Observation of surface-guided waves in holey hypersonic phononic crystal

Sarah Benchabane,<sup>a)</sup> Olivier Gaiffe, Gwenn Ulliac, Roland Salut, Younes Achaoui, and Vincent Laude

*Institut FEMTO-ST, Université de Franche-Comté, CNRS, 32 Avenue de l'Observatoire, F-25044 Besançon Cedex, France*

(Received 18 January 2011; accepted 8 April 2011; published online 28 April 2011)

We observe experimentally the propagation of surface-guided waves in a hypersonic phononic crystal, both in the radiative and nonradiative regions of the spectrum. Combining electrical measurements in reflection and transmission as well as optical maps of the surface displacement, a band gap extending from 0.6 to 0.95 GHz is identified in a square lattice array of 1  $\mu\text{m}$  radius air holes milled in lithium niobate. The optical measurements reveal the transmission of surface-guided waves above the band gap, well inside the sound cone. © 2011 American Institute of Physics. [doi:10.1063/1.3583982]

When phononic crystals (PCs) were introduced in the early 1990s, their ability to prohibit elastic wave propagation in a given frequency range was first put forward in the case of bulk waves.<sup>1,2</sup> The potential behind these artificial materials, obtained by imposing a strong periodic modulation in density and elastic constants, was immediately obvious: PCs offered unprecedented ways of blocking and steering the course of elastic waves. Radio-frequency wireless systems rapidly arose as one of their natural fields of applications and hypersonic PCs in the appropriate gigahertz frequency range, that is, exhibiting features at the submicron scale, were again initially demonstrated for bulk waves.<sup>3,4</sup> But in this subfield of telecommunications, acoustic waves confined to the surface and their combination with piezoelectric solid occupy a prominent position. Efficient electrical sources can indeed be found in interdigital transducers (IDTs) and single-mode operation is made possible by the very nature of the generated surface waves.

A series of works then focused on investigating the interaction between these waves and PCs, which led to theoretical papers demonstrating that complete surface wave band gaps can be obtained in perfect two-dimensional (2D) PCs.<sup>5–8</sup> Practically however, it is impossible to create infinitely deep holes and PC samples are rather in the form of a PC layer standing on a semi-infinite substrate. Although transmission below and strong attenuation within the band gap were experimentally observed, significant energy loss was reported at higher frequencies,<sup>9–12</sup> even before the surface-guided waves actually exit the band gap. These high-frequency modes are located above the sound line—defined by the dispersion relation of the bulk mode with the lowest velocity—and are hence subject to radiation to the substrate. An increasing research effort has been since then driven toward phononic slabs and the confinement offered by membranes<sup>13–21</sup> as a natural way to avoid radiation to the bulk. This benefit is however offset by the difficulty to control the number of modes that propagate in an adequately proportioned membrane. There is therefore a genuine trade-off between confinement and single-mode operation and both surface and plate wave solutions remain worth being explored.

In this letter, we investigate surface-guided mode propagation in a hypersonic PC made of air holes milled in a piezoelectric matrix. Combining electrical measurements in transmission and reflection, the bandgap can be separated from the radiative region. Optical measurements confirm the presence of the bandgap but also reveal a clear transmission of surface waves lying within the sound cone, hence showing that configurations do exist where radiation losses can be made acceptable.

The PC structure is described in Fig. 1 and was obtained by patterning an X-cut lithium niobate substrate by focused ion beam milling.<sup>22</sup> The air holes were arranged according to a square lattice, with a period of 2.2  $\mu\text{m}$ . Each hole is about 2.3  $\mu\text{m}$  in depth and presents smooth sidewalls with a slope angle of the order of 85°, which is a definite improvement compared to the 75° achieved through reactive ion etching.<sup>23</sup> The filling fraction was kept close to 64%, as this value allows opening a complete bandgap for surface waves in this air/LiNbO<sub>3</sub> structure,<sup>7,10</sup> theoretically ranging from 0.66 to 1.1 GHz for a crystal exhibiting infinitely deep and perfectly cylindrical air holes.

Electroacoustic delay lines were used for the excitation and detection of surface-guided modes, as illustrated in Fig. 1(a). They consist of a pair of 160-finger chirped IDTs exhibiting a linear variation in the electrical period along their length, allowing for a broadband emission over more than an octave. Only a couple of identical PCs, surrounded by two different sets of transducers, were then required for a full characterization of the expected phononic bandgap, as opposed to eight pairs of transducers in Ref. 10. The mechanical period of the transducers ranges from 1.7 to 3.75  $\mu\text{m}$  and from 1.25 to 2.75  $\mu\text{m}$ . They are 435  $\mu\text{m}$  and 320  $\mu\text{m}$  long, respectively, and separated by 80  $\mu\text{m}$  of free space.

Transmission through delay lines devoid of any PC were taken as a reference in order to get a transmittance for the PC samples. The corresponding experimental data are reported in Fig. 1(c). A good overlap between the two signals can be observed at frequencies below 650 MHz. Beyond this frequency, the electrical response is strongly attenuated, with an extinction ratio of the order of 13 dB. Partial retransmission occurs from a frequency of about 1 GHz but there is no undisputable evidence of surface modes above the bandgap.

<sup>a)</sup>Electronic mail: sarah.benchabane@femto-st.fr.

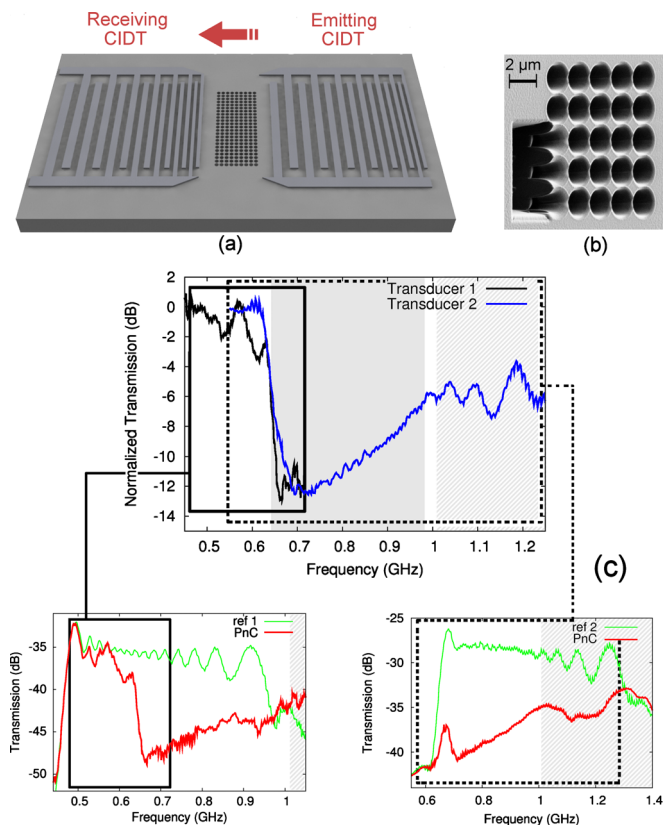


FIG. 1. (Color online) (a) Schematic of the 2D PC made of air holes in a lithium niobate matrix used in this experiment. The period of the crystal is around  $2.2 \mu\text{m}$ , for a hole radius of  $1 \mu\text{m}$ . The crystal is surrounded by a pair of chirped IDTs. (b) Scanning electron microscope image of the square lattice crystal. (c) Normalized transmittance for surface-guided modes propagating through the PC. The gray area delimits the band gap position and the hatched area highlights the radiative zone lying beyond the sound line. The transmission responses of each PC and of the two electro-acoustic delay lines used as references are also plotted.

Reflection measurements, reported in Fig. 2, provide us with complementary information. Introducing the PC results in additional oscillations in the reflection, as can be seen in Fig. 2(a). This can be accounted for as follows: within the bandgap, we expect the PC to behave as a mirror reflecting incident waves. Since the emitting transducer is chirped, a particular frequency is preferentially emitted and detected around a specific position along the transducer. The round-trip time or distance corresponding to the sequence generation-reflection-detection must then follow an inverse-linear law as a function of frequency. The propagation phase also follows the same law, which causes the appearance of a sequence of maxima (constructive interference) and minima (destructive interference) in the reflection. The round-trip distance for each frequency component can thus be estimated from the frequency spacing between two successive oscillations.

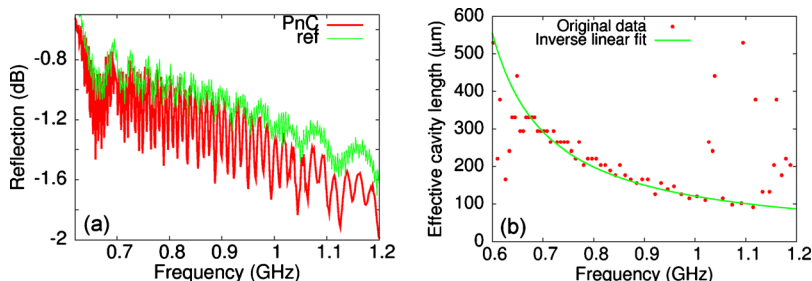


FIG. 2. (Color online) (a) Reflection vs frequency in the 0.6 to 1.2 GHz range, that encompasses the bandgap. The reference signal is also shown. (b) Round-trip distance, worked out from the reflection measurements. A frequency band ranging from about 0.65 to 1 GHz clearly exhibits an inverse linear behavior.

The results obtained for the higher frequency transducer are reported in Fig. 2(b). In the 0.65 to 1 GHz frequency range, this quantity follows well the theoretical inverse-linear law. Outside it, strong fluctuations are observed instead. Since the above simple model works only if the PC acts as a nearly perfect mirror, we infer that the band gap extends at least from 0.65 to 1 GHz. We can further note that in this frequency range the round-trip distance varies from 100 to  $350 \mu\text{m}$ , which compares well with the sample layout.

Optical mapping of the displacement fields in the PC (Ref. 12) was then carried out using an optical heterodyne interferometer,<sup>24</sup> here only allowing amplitude detection. A single IDT was used as a surface wave source. Maps of the out-of-plane displacement were taken for areas encompassing the PC and some free space at the entrance and output. The dimensions of the scan are  $20 \times 90 \mu\text{m}^2$  and the lateral scanning step is  $0.5 \mu\text{m}$  in both directions. Only the center of the acoustic beam was scanned, as the beam is supposed to be invariant along the transducer finger length when remaining well inside the acoustic aperture. Measurements were performed at frequencies supposedly lying before, within and after the bandgap and are displayed in Fig. 3. As expected, below the bandgap, e.g., at 540 MHz, the elastic wave passes through the crystal and is almost unaltered by the PC. In contrast, a standing wave pattern is clearly observed at 660 MHz (bandgap edge) and at 800 MHz (center), confirming that both frequencies lie within the bandgap for surface guided modes. The wave penetration length inside the PC is higher at the band edge than at the central frequency and up to 25% of the elastic energy is still transmitted at 660 MHz. At 800 MHz, a plot of the averaged cross-section of the surface motion reveals an exponential decrease in the wave amplitude inside the crystal, resulting in an output wave amplitude within the noise level. The most striking results are observed at higher frequencies: at 1.05 GHz, at which frequency the electrical transmittance is weak, the optical scan clearly demonstrates that transmission occurs above the bandgap. The average amplitude at the output was evaluated to be around 0.17 nm, versus 0.22 nm for the incident wave, resulting in an amplitude transmission close to 75%. This result shows that configurations do exist where the sound line limit can be partly overcome. The sound cone designates a frequency region where leakage from surface to bulk modes can happen, but this does not imply that surface-guided wave propagation is fully prohibited in this part of the spectrum. In practical applications, radiation to the bulk can still prevent from taking full advantage of the PC capabilities over the entire frequency range of operation, but the band gaps observed for surface-guided modes lying below the sound line, i.e., here below 1.01 GHz, remain perfectly valid. The frequency range outside the sound cone should

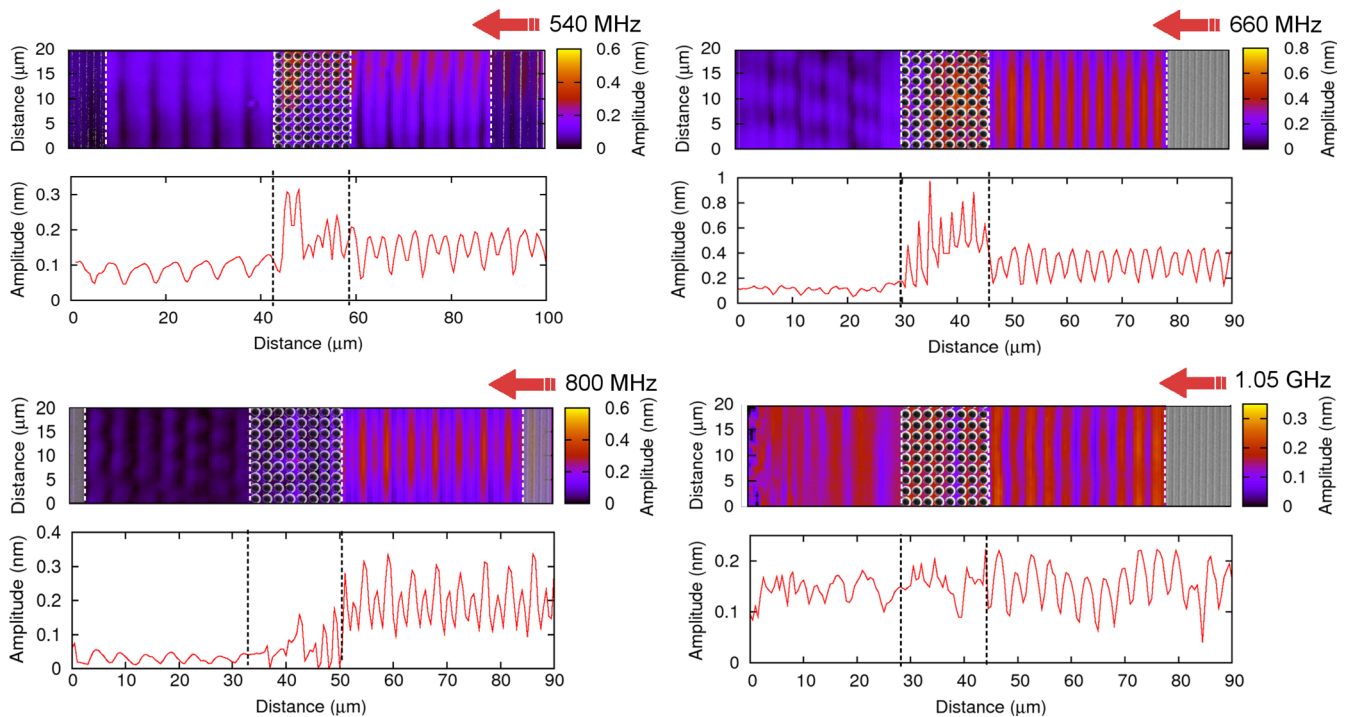


FIG. 3. (Color online) Measured elastic wave fields propagating through the PCs for excitation frequencies at the edge of (660 MHz), below (540 MHz), within (880 MHz) and above (1.05 GHz) the bandgap. The emitting transducer stands at the right hand side. A scanning electron microscope image of the crystal and transducers is overlaid to the field map. The amplitude data are averaged in the  $y$ -direction and the line profiles along the propagation direction are displayed.

hence be favored for the design of efficient waveguides or high-Q cavities.

In conclusion, we demonstrated not only that bandgaps for surface-guided waves can be obtained at near-gigahertz frequencies but also that a clear transmission of the signal can be observed for modes lying within the sound cone. By measuring the electrical reflection, we could estimate the frequency bandgap, although transmission measurements were corrupted by radiation to the bulk. Optical measurements of the out-of-plane wave motion confirm that the crystal behaves as a perfect mirror in the band gap and that transmission is possible below and significantly above the forbidden frequency band, even for frequencies inside the sound cone.

This work has been carried out within Project No. ANR-09-NANO-004 (phoxcry) funded by ANR (P3N2009) and received partial support from the European Commission Seventh Framework Programme (FP7) under Grant Agreement No. 233883 (TAILPHOX). The authors would like to thank Valérie Pétrini for technical assistance.

- <sup>1</sup>M. S. Kushwaha, P. Halevi, L. Dobrzynski, and B. Djafari-Rouhani, *Phys. Rev. Lett.* **71**, 2022 (1993).
- <sup>2</sup>M. Sigalas and E. N. Economou, *Solid State Commun.* **86**, 141 (1993).
- <sup>3</sup>T. Gorishnyy, C. K. Ullal, M. Maldovan, G. Fytas, and E. L. Thomas, *Phys. Rev. Lett.* **94**, 115501 (2005).
- <sup>4</sup>W. Cheng, J. Wang, U. Jonas, G. Fytas, and N. Stefanou, *Nature Mater.* **5**, 830 (2006).
- <sup>5</sup>Y. Tanaka and S. Tamura, *Phys. Rev. B* **58**, 7958 (1998).
- <sup>6</sup>T. Wu, Z. Huang, and S. Lin, *Phys. Rev. B* **69**, 094301 (2004).

- <sup>7</sup>V. Laude, M. Wilm, S. Benchabane, and A. Khelif, *Phys. Rev. E* **71**, 036607 (2005).
- <sup>8</sup>A. Khelif, Y. Achaoui, S. Benchabane, V. Laude, and B. Aoubiza, *Phys. Rev. B* **81**, 214303 (2010).
- <sup>9</sup>T. Wu, L. Wu, and Z. Huang, *J. Appl. Phys.* **97**, 094916 (2005).
- <sup>10</sup>S. Benchabane, A. Khelif, J.-Y. Rauch, L. Robert, and V. Laude, *Phys. Rev. E* **73**, 065601(R) (2006).
- <sup>11</sup>D. M. Profunser, O. B. Wright, and O. Matsuda, *Phys. Rev. Lett.* **97**, 055502 (2006).
- <sup>12</sup>K. Kokkonen, M. Kaivola, S. Benchabane, A. Khelif, and V. Laude, *Appl. Phys. Lett.* **91**, 083517 (2007).
- <sup>13</sup>A. Khelif, B. Aoubiza, S. Mohammadi, A. Adibi, and V. Laude, *Phys. Rev. E* **74**, 046610 (2006).
- <sup>14</sup>B. Bonello, C. Charles, and F. Ganot, *Appl. Phys. Lett.* **90**, 021909 (2007).
- <sup>15</sup>F.-L. Hsiao, A. Khelif, H. Moubchir, A. Choujaa, C.-C. Chen, and V. Laude, *Phys. Rev. E* **76**, 056601 (2007).
- <sup>16</sup>T.-T. Wu, Z.-G. Huang, T.-C. Tsai, and T.-C. Wu, *Appl. Phys. Lett.* **93**, 111902 (2008).
- <sup>17</sup>Y. Pennec, B. Djafari-Rouhani, H. Larabi, J. O. Vasseur, and A. C. Hladky-Hennion, *Phys. Rev. B* **78**, 104105 (2008).
- <sup>18</sup>I. El-Kady, R. H. Olsson, and J. G. Fleming, *Appl. Phys. Lett.* **92**, 233504 (2008).
- <sup>19</sup>S. Mohammadi, A. Eftekhar, A. Khelif, W. Hunt, and A. Adibi, *Appl. Phys. Lett.* **92**, 221905 (2008).
- <sup>20</sup>S. Mohammadi, A. Eftekhar, W. Hunt, and A. Adibi, *Appl. Phys. Lett.* **94**, 051906 (2009).
- <sup>21</sup>M. F. Su, R. H. Olsson III, Z. C. Leseman, and I. El-Kady, *Appl. Phys. Lett.* **96**, 053111 (2010).
- <sup>22</sup>F. Lacour, N. Courjal, M.-P. Bernal, A. Sabac, C. Bainier, and M. Spajer, *Opt. Mater.* **27**, 1421 (2005).
- <sup>23</sup>S. Benchabane, L. Robert, J.-Y. Rauch, A. Khelif, and V. Laude, *J. Appl. Phys.* **105**, 094109 (2009).
- <sup>24</sup>P. Vairac and B. Cretin, *Opt. Commun.* **132**, 19 (1996).